Clinical Cancer Research

Tumor Growth Inhibition by Olaparib in *BRCA2* Germline-Mutated Patient-Derived Ovarian Cancer Tissue Xenografts

Ursula Kortmann, Jessica N. McAlpine, Hui Xue, et al.

Clin Cancer Res 2011;17:783-791. Published OnlineFirst November 19, 2010.

Published OnlineFirst November 19, 2010; DOI:10.1158/1078-0432.CCR-10-1382

Cancer Therapy: Preclinical

Clinical Cancer Research

Tumor Growth Inhibition by Olaparib in *BRCA2* Germline-Mutated Patient-Derived Ovarian Cancer Tissue Xenografts

Ursula Kortmann[1,2], Jessica N. McAlpine[3], Hui Xue[2], Jun Guan[2], Gavin Ha[4], Sophie Tully[5], Sharaz Shafait[5], Alan Lau[6], Aaron N. Cranston[5], Mark J. O'Connor[6], David G. Huntsman[1,7], Yuzhuo Wang[2,8], and C. Blake Gilks[7]

Abstract

Purpose: Most patients with ovarian carcinomas succumb to their disease and there is a critical need for improved therapeutic approaches. Carcinomas arising in *BRCA* mutation carriers display defective DNA double-strand break repair that can be therapeutically exploited by inhibition of PARP-1, a key enzyme in the repair of DNA single-strand breaks, creating synthetic lethality in tumor cells.

Experimental Design: To investigate synthetic lethality *in vivo*, we established a *BRCA2* germline-mutated xenograft model that was developed directly from human ovarian cancer tissue, treated with the PARP inhibitor olaparib (AZD2281) alone and in combination with carboplatin.

Results: We show that olaparib alone and in combination with carboplatin greatly inhibit growth in *BRCA2*-mutated ovarian serous carcinoma. This effect was not observed in a serous carcinoma with normal *BRCA* function, showing a specific antitumor effect of olaparib in mutation carriers. Immunohistochemistry (cleaved caspase-3 and Ki-67 stains) of remnant tissue after olaparib treatment revealed significantly decreased proliferation and increased apoptotic indices in these tumors compared with untreated controls. Furthermore, olaparib-treated tumors showed highly reduced PARP-1 activity that correlated with olaparib levels.

Conclusions: We established a *BRCA2*-mutated human ovarian cancer xenograft model suitable for experimental drug testing. The demonstrated *in vivo* efficacy of olaparib extends on the preclinical rationale for further clinical trials targeting ovarian cancer patients with *BRCA* mutations. *Clin Cancer Res; 17(4); 783–91. ©2010 AACR.*

Introduction

Ovarian cancer is the fifth leading cause of cancer death in North American women and the most fatal gynecological cancer (1). Approximately 10% of all ovarian cancers are hereditary and of these, more than 90% are associated with *BRCA1* or *BRCA2* germline mutations (2). In addition, a smaller number of nonhereditary ovarian cancers show somatic *BRCA* mutations, and functional loss of *BRCA1* through promoter methylation is commonly observed. These changes together result in the *BRCA* deficiency associated with high-grade serous ovarian carcinoma (HGSC), the most frequent histologic subtype in epithelial ovarian cancer (3, 4). Patients with *BRCA* germline mutations treated with platinum-based therapy regimens have a survival advantage compared with nonhereditary ovarian carcinoma of HGSC subtype (5). Regardless, the majority of patients with HGSC relapse and ultimately die from their disease, therefore development of effective first-line therapies is critical.

BRCA1 and *BRCA2* encode tumor suppressor proteins that are part of a multicomponent complex (RAD51 complex) involved in the repair of DNA double-strand breaks (DSBs) and collapsed replication forks by the process of homologous recombination, and are therefore essential for maintaining genomic stability (6). This genetic defect in the DNA repair pathway of affected tumors can be exploited by using poly(ADP)-ribose polymerase (PARP) inhibitors to induce selective tumor cytotoxicity while sparing normal cells. The most abundant member of the PARP family, PARP-1, plays a crucial role in the repair of DNA

Authors' Affiliations: [1]Department of Pathology, British Columbia Cancer Agency and University of British Columbia; [2]Living Tumor Laboratory, British Columbia Cancer Agency; [3]Division of Gynecologic Oncology, Department of Obstetrics and Gynecology, University of British Columbia; [4]Department of Molecular Oncology, British Columbia Cancer Research Centre, Vancouver, British Columbia, Canada; [5]KuDOS Pharmaceuticals Ltd., Cambridge, United Kingdom; [6]AstraZeneca, Cancer Bioscience, Cheshire, United Kingdom; [7]Department of Pathology, Genetic Pathology Evaluation Centre, Vancouver General Hospital, Centre for Translation and Applied Genomics, British Columbia Cancer Agency and University of British Columbia; and [8]Department of Urologic Sciences, The Prostate Centre at Vancouver General Hospital, University of British Columbia, Vancouver, British Columbia, Canada

Note: S. Tully, S. Shafait, and A.N. Cranston are former KuDOS employees.

Corresponding Author: C. Blake Gilks, Department of Pathology and Laboratory Medicine, University of British Columbia, Vancouver General Hospital, 910 West 10th Avenue, Vancouver, BC V5Z 1M9, Canada. Phone: 604-875-4901; Fax: 604-875-4497. E-mail: blake.gilks@vch.ca

doi: 10.1158/1078-0432.CCR-10-1382

Published OnlineFirst November 19, 2010; DOI:10.1158/1078-0432.CCR-10-1382

Translational Relevance

The efficacy of conventional platinum-based chemotherapy for high-grade serous carcinoma is limited; most patients show an initial response to treatment but upon relapse, response rates to platinum progressively diminish and they ultimately die of progressive disease. By capitalizing on the genetic defect in DNA double-strand repair in serous carcinomas with *BRCA* loss, through targeting of DNA single-strand repair with the poly(ADP)-ribose polymerase (PARP)-inhibitor olaparib, selective tumor cytotoxicity can be induced while sparing normal cells. We show that olaparib therapy results in tumor cell death in a human ovarian carcinoma xenograft with a *BRCA2* mutation, but not in a xenograft with normal *BRCA*1 and *BRCA2*, and the effects of olaparib are increased with concomitant carboplatin treatment. This study describes a clinically relevant model of serous ovarian carcinoma for drug testing, and provides a rationale for trials of combined PARP-inhibitor/platinum chemotherapy for serous carcinomas with *BRCA* loss.

single-strand breaks (SSBs) via the base excision repair pathway. Inhibition of PARPs leads to the accumulation of DNA SSBs, which can lead to DNA DSBs at replication forks. This synthetically lethal effect of *BRCA1*/*BRCA2* mutation and interventional PARP-1 inhibition, leading to deficiency in both the SSB and DSB pathways, has been shown to enhance the cytotoxic effects of ionizing radiation and DNA damaging chemotherapy agents, such as DNA cross-linking agents, alkylating agents, and topoisomerase I inhibitors (7–9).

Most HGSC, regardless of the *BRCA* mutation status, has already spread beyond the confines of the ovary at diagnosis and therefore management involves surgical debulking, followed by chemotherapy with carboplatin and a taxane (10, 11). To improve response rates and treatment-free intervals, and to offer treatment alternatives to these existing therapies, PARP inhibitors have been recently introduced and tested in early clinical trials as single agents or as part of combination therapies in patients with advanced solid tumors (12–14). These trials were prompted by convincing preclinical assays showing that cell lines lacking wild-type *BRCA1* or *BRCA2* were extremely sensitive to potent PARP inhibitors compared with heterozygous mutant or wild-type cells (15–18).

Recently, the orally active PARP inhibitor, olaparib (AZD2281), was evaluated as a single-agent therapy in humans, showing clinical antitumor activity in *BRCA*-associated cancers (primarily ovarian carcinomas; ref. 14).

In this study, we present a *BRCA2*-mutated human ovarian cancer tissue explant xenograft model to investigate the therapeutic response to olaparib as a single agent and in combination with chemotherapy.

Materials and Methods

Transplantable patient-derived ovarian cancer tissue lines

Ovarian tumor tissue specimens were obtained, with informed consent, from patients undergoing surgical staging for primary ovarian cancer at Vancouver General Hospital, Vancouver, BC, Canada. Fresh tumor tissue was cut into small pieces and grafted under the renal capsule of female NOD-SCID mice for subsequent serial transplantation and characterization as previously described (19). Animal care and experiments were carried out in accordance with the guidelines of the Canadian Council on Animal Care, Ottawa, ON, Canada and human tissue specimens managed per protocol approved by the University of British Columbia Clinical Research Ethics Board, Vancouver, BC, Canada. Treatment response (olaparib, carboplatin, and combination) was tested in LTL247, a tumor line derived from a patient with a known *BRCA2* germline mutation (exon 11 c4848–4849 delAA). Pathology review of the original tumor specimen confirmed HGSC subtype. LTL258 (*BRCA* wild type) developed from the HGSC tumor of a different patient was selected as a paired control.

BRCA mutation analysis

BRCA2 coding sequence mutations were confirmed by whole transcriptome RNA sequencing (RNA-seq) as previously described (20) and direct sequencing (ABI, 3130xl Genetic Analyzer) in original patient tumor and in the later passages of tumor line LTL247 (primer sequences exon 11: *BRCA2* forward aaagaccctaaagtacagagagg, *BRCA2* reverse cggcccgccgcccccgcccgatttattctttctggttgaccatc). Wild-type status of *BRCA* 1 and 2 in LTL 258 were confirmed using reference primers as described before (4).

Affymetrix SNP 6.0 arrays were used to determine the copy number of chromosome 13q harboring the *BRCA2* locus for the original patient tumor and a later generation xenograft of LTL247. The arrays were normalized using CRMAv2 (21) and default settings for performing allelic-crosstalk calibration, probe sequence effects normalization, probe-level summarization, and PCR fragment length normalization. Log ratios were then computed by normalizing against a reference generated using a normal dataset of 270 HapMap samples obtained from Affymetrix. Segmentation was performed using a modified 11-state hidden Markov model (http://compbio.bccrc.ca/?page_id = 401) derived from CNA-HMMer (20). Segment calls were generated according to 5 somatic states (homozygous deletion, hemizygous deletion, gain, amplification, and high-level amplifcation), 5 analogous germline states, and neutral copy number.

Olaparib efficacy studies

The structure and activity of olaparib (AZD2281, KU-0059436) has been previously described (9, 14, 17, 18). Olaparib was solubilized in DMSO and diluted to 5 mg/mL with PBS containing 10% (w/v) 2-hydroxy-propyl-beta-cyclodextrin (Sigma).

Published OnlineFirst November 19, 2010; DOI:10.1158/1078-0432.CCR-10-1382

After 2 tumor doubling times (DT for LTL247:10 days and DT for LTL258: 16 days), reaching a calculated average volume of 16.6 mm^3, the animals were randomized into 4 treatment groups (4–6 mice/group; 2 grafts/kidney): (1) olaparib alone, (2) carboplatin alone, (3) both agents, and (4) vehicle control. LTL247 mice were treated for 4 weeks and LTL258 mice were treated for 5 weeks. Olaparib was dosed i.p. (50 mg/kg) once daily for 5 days × 4 weeks for LTL247 and ×5 weeks for LTL258 (17, 18); carboplatin (Novopharm Ltd.) was dosed i.p. (50 mg/kg) once weekly ×4 weeks for LTL247 and ×5 weeks for LTL258 (18). Mice were provided with food and water *ad libitum* and monitored daily for changes in general health, including body weight loss, diarrhea, food–water intake, appearance, and behavior. Tumors were harvested on day 29 and 35 for LTL247 and LTL258, respectively, 2 hours after last dosing.

Tumor burden was determined at necropsy as previously described (19). Mean tumor volume (mm^3) ± (SD) was calculated and growth inhibition (GI) was reported as the percentage decrease of tumor volume compared with the vehicle control. Individual group comparisons were performed using independent student *t*-tests and overall group comparisons were performed using one-way ANOVA. Results with $P < 0.05$ were reported as significant.

Immunohistochemistry (proliferation and apoptotic indices)

Immunohistochemistry was performed on 5 μm paraffin-embedded tissue sections using TUNEL assays (ApopTag Apoptosis Detection Kit, Chemicon) and a monoclonal MIB1 antibody (Dako, dilution 1:50) directed against the Ki-67 antigen as previously described (19).

For cleaved caspase-3 staining, 4 μm thick sections were cut and immunostained on a Ventana Discovery XT staining system (Ventana Medical Systems). Sections were deparaffinized in xylene, dehydrated through 3 alcohol changes, and transferred to Ventana Wash solution. Endogenous peroxidase activity was blocked in 3% hydrogen peroxide. Antigen retrieval was performed in cell conditioner 1 and slides were incubated with anti-cleaved caspase-3 rabbit monoclonal antibody (1:100 dilutions, clone 5A1E, Cell Signaling Technology) for 60 minutes. Finally, sections were incubated with the UltraMap anti-rabbit HRP-conjugate and ChromoMap detection system (Ventana Medical Systems), counterstained with hematoxylin, dehydrated, cleared, and mounted.

The Ki-67 proliferation index (PI) was determined on a minimum of two randomly selected high-power fields (400× magnification) containing representative sections of tumor tissue and calculated as the percentage of positively stained tumor cells to total tumor cells. The apoptotic index (AI) using cleaved caspase-3 and TUNEL stains was calculated as the percentage of positively stained apoptotic tumor cells to total tumor cells by counting at least three high-power fields (at 400× magnification). Areas with extensive necrosis were avoided.

Compound level quantification and PARP-1 activity determination in *BRCA2*$^{-/-}$ tumor tissues

To show the specific PARP inhibitory effect of olaparib therapy, we determined the *ex vivo* PARP-1 activity in relation to the drug compound levels in 5 *BRCA2*$^{-/-}$ xenografts of LTL247after 4 weeks of treatment and six untreated controls.

Olaparib levels were analyzed by ultra-performance liquid chromatography–tandem mass spectrometry (UPLC–MS/MS). Tumors were weighed, homogenized in 3 volumes of PBS, and samples extracted using solid phase extraction. Chromatographic separation was by gradient elution using an Acquity BEH Phenyl (5.0 × 2.1 mm, 1.7 μm) column coupled to a Sciex API 2000 with electrospray ionization (ESI) in positive ion mode using multiple reaction monitoring of ions 435.32 to 281.10 m/z. Calibration standards (10–5,000 ng/mL) and quality control samples were prepared in mouse plasma and tumor homogenate.

PARP-1 activity within tumor samples was analyzed using an *ex vivo* activation assay as previously described (9).

Results

Model characterization

We selected a tumor line originating from a patient with known heterozygous *BRCA2* germline mutation. This mutation could be characterized as a 2 base pair deletion frameshift mutation in *BRCA*2 exon 11 using the patients constitutional DNA (peripheral blood; Fig. 1). Copy number analysis of the patient tumor and the late generation xenograft revealed a hemizygous deletion of the *BRCA*2 locus with loss of heterozygosity. Accordingly, direct sequencing showed a homozygous state of the frameshift mutation in the primary and xenograft tumors. RNA-seq confirmed exclusive expression of the mutated allele that was supported by 2 reads (data not shown). In summary, this homozygous frameshift mutation can be considered as a loss of function mutation. In contrast, tumor line LTL258 did not show *BRCA1* or *BRCA2* mutations (data not shown).

Olaparib inhibits growth of *BRCA2*$^{-/-}$ ovarian cancer tissue xenografts

All 39 mice included in the study were available for evaluation and measurement of tumors on harvest day. On macroscopic inspection, LTL247$^{BRCA2-/-}$ xenografts treated for 4 weeks with vehicle showed, on average, markedly enlarged tumor masses. This was confirmed on microscopic evaluation, with H&E staining identifying viable cancer cells (Fig. 2, middle). In contrast, olaparib-treated tumors showed much smaller tumor masses, lower overall cell numbers, increased numbers of dead cells, and more cells with enlarged cellular and nuclear structures than controls (Fig. 2, right). Morphometric measurements revealed significant differences in tumor mass between treatment groups tested with simultaneous comparison of means (ANOVA; $P = 9.78e\text{-}14$). Individual group comparisons showed that treatment with olaparib alone markedly inhibited growth of the LTL247$^{BRCA2-/-}$ HGSC line

Published OnlineFirst November 19, 2010; DOI:10.1158/1078-0432.CCR-10-1382

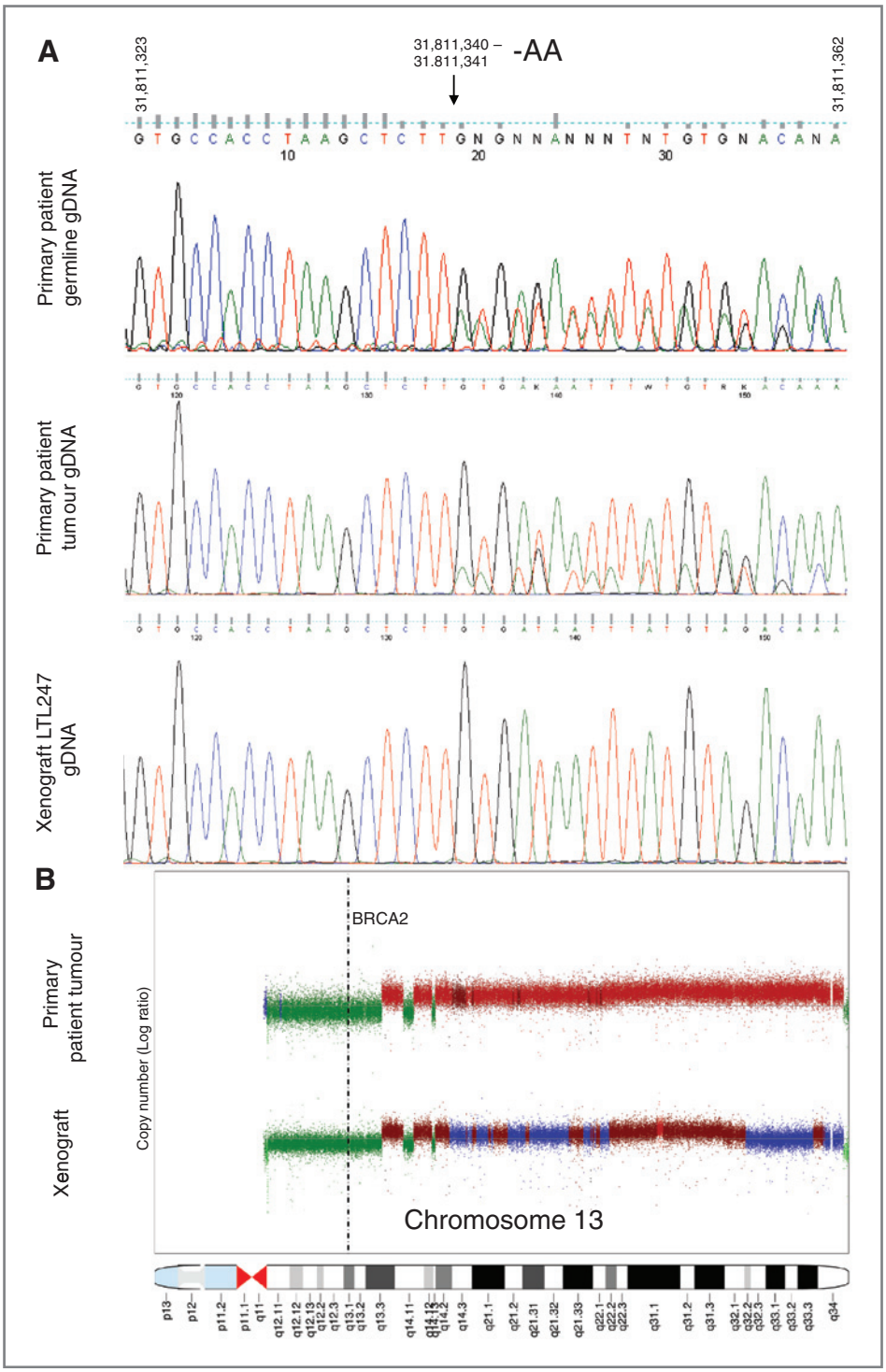

Figure 1. A, direct sequencing of the 2 base pair deletion frameshift mutation in *BRCA2* exon 11. Top panel, patient germline gDNA showing a heterozygous deletion AA; middle panel, primary patient tumor gDNA showing a homozygous deletion with likely contamination by stromal cells; bottom panel, matching late generation xenograft gDNA showing a homozygous deletion without contamination (xenograft tumor with less than 1% mouse stroma cells). B, Affymetrix SNP6.0 data comparing primary tumor and xenograft samples. Each probe is represented as a point in the plot, where the *y*-axis is log *R* and the *x*-axis is chromosome position (bp). Hidden Markov Model (HMM) discrete copy number predictions are represented by color coding: homozygous deletion (light green), hemizygous deletion (dark green), neutral (blue), gain (dark red), and amplification (light red). In both samples, *BRCA2* (dotted black line) is contained within a hemizygous deletion region.

compared with the untreated controls (19.7 $mm^3 \pm 25.0$ mm^3 vs. 97.3 $mm^3 \pm 72.6$ mm^3; GI 79.8%; $P = 3.1e\text{-}5$), although the tumor volume on average was still minimally larger than the calculated volume on the first day of treatment. Treatment with carboplatin alone also resulted in significant GI (4.4 $mm^3 \pm 7.4$ mm^3 vs. 97.3 $mm^3 \pm 72.6$ mm^3; GI 95.5%; $P = 2.1e\text{-}6$), whereas combination of olaparib and carboplatin showed the best treatment response (1.2 $mm^3 \pm 1.4$ mm^3 vs. 97.3 $mm^3 \pm 72.6$ mm^3; GI 98.8%; $P = 1.29e\text{-}6$; Fig. 3A, left). Carboplatin and carboplatin + olaparib-treated tumors resulted in very small residual explant tissue consisting mostly of scar tissue

Published OnlineFirst November 19, 2010; DOI:10.1158/1078-0432.CCR-10-1382

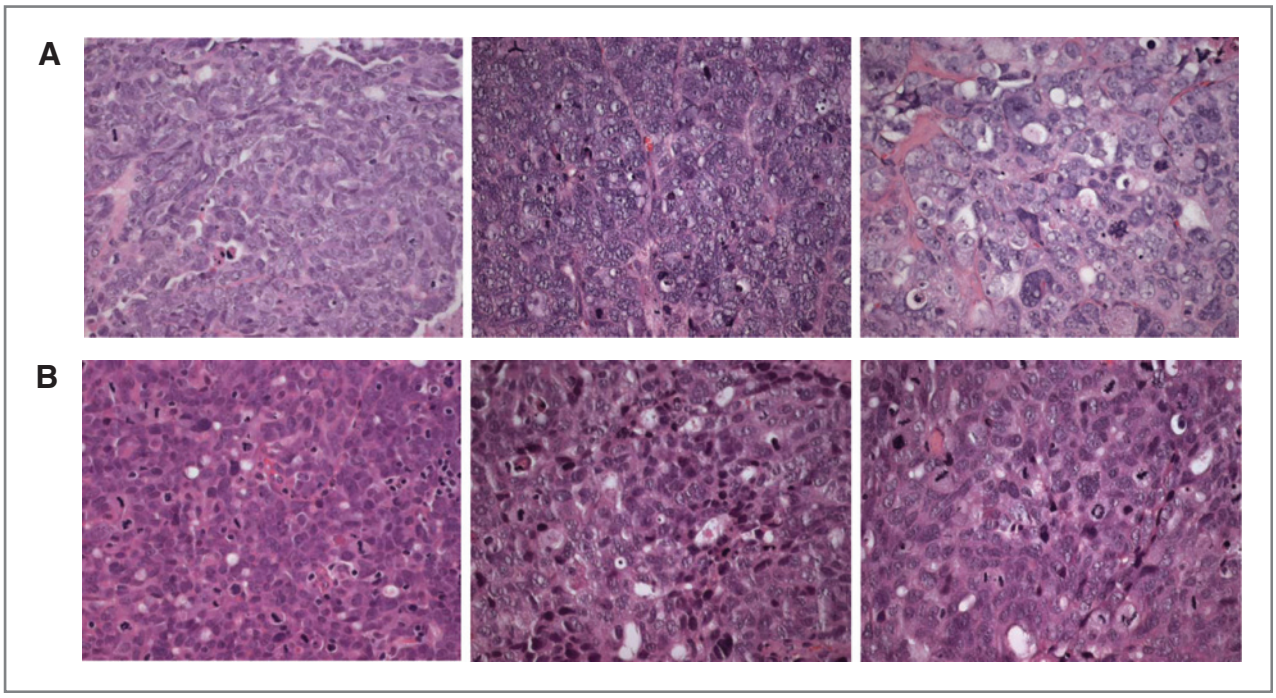

Figure 2. H&E staining (400× magnification) of tumor sections from A, *BRCA2*$^{-/-}$ xenograft LTL247. Left, primary patient tumor; middle, untreated control xenograft; right, olaparib-treated xenograft. B, *BRCA1*$^{+/+}$, *BRCA2*$^{+/+}$ wild-type xenograft LTL258. Left, primary patient tumor; middle, untreated control xenograft; right, olaparib-treated xenograft.

(not shown). After regrafting the 2 largest residual tumors of the olaparib alone and the combination treatment group as well as 2 tumors of the control group, different latency times were observed before regrowth: both control tumors reconstituted to palpable size after 6 weeks while one of the olaparib alone treated tumors reconstituted after 12 months. In contrast, the second olaparib-treated tumor and the combination-treated tumors never expanded in size until the mice had to be euthanized after 14–18 months.

BRCA wild-type LTL258$^{BRCA1+/+,BRCA2+/+}$ xenografts did not show significant GI with olaparib compared with vehicle-treated mice (90.1 mm^3 ± 66.4 mm^3 vs. 112.9 mm^3 ± 90.2 mm^3; GI 20.2%; $P = 0.403$), whereas treatment with carboplatin (14.9 mm^3 ±12.7 mm^3 vs. 112.9 mm^3 ± 90.2 mm^3; GI 86.8%; $P = 0.0008$) and combination therapy of carboplatin and olaparib (34.0 mm^3 ± 25.6 mm^3 vs. 112.9 mm^3 ± 90.2 mm^3; GI 69.9%; $P = 0.004$) significantly reduced tumor size (Fig. 3A, right).

Toxicity evaluation

Only 4 of all the treated animals showed substantial loss of body weight (>10%), 3 mice bearing tumor LTL258, and 1 bearing LTL247. Two of the mice received vehicle only, one carboplatin, and one the combination treatment. No gross changes in food–water intake, appearance, or behavior were observed, indicating that the treatments were well tolerated. Particularly, the addition of olaparib to carboplatin did not significantly increase weight loss compared with carboplatin single agent treatment in the LTL247$^{BRCA2-/-}$ tumor line (carboplatin average weight gain 0.4% vs. combination average weight loss 1.6%; $P = 0.5$). Similarly, no statistically significant increase of weight loss was observed in the *BRCA* wild-type line LTL258 (carboplatin average weight loss 5.7% vs. combination average weight loss 6.6%, $P = 0.9$).

Olaparib-treated tumors exhibit decreased proliferation and increased apoptosis

Immunohistochemical analysis of Ki-67-stained tissue sections from 4 randomly selected LTL247$^{BRCA2-/-}$ xenografts, treated for 4 weeks with olaparib (Fig. 4A, right), showed a significantly lower number of proliferating cells compared with 4 untreated LTL247$^{BRCA2-/-}$ control xenografts (Fig. 4A, left). On average, the percentage of proliferating cells per high-power field was 1.9-fold lower in the olaparib-treated tumors [29.5% ± 14.1% (SD) vs. 55.7% ± 10.3% (SD); $P = 0.0006$). In contrast, olaparib-treated xenografts of the *BRCA* competent tumor line did not show significant reduction of proliferating cells compared with untreated control xenografts [19.1% ± 6.4% (SD) vs. 20.4% ± 5.7% (SD); $P = 0.7$; Fig. 4D, right and left).

Cleaved caspase-3 stains of 3 representative olaparib-treated LTL247$^{BRCA2-/-}$ tissue sections (Fig. 4C, right) displayed a significantly higher number of apoptotic cells than untreated control xenografts (Fig. 4C, left). On an average, the AI per high-power field was 3.8-fold increased in the olaparib-treated tumors [3.1% ± 1.8%

Published OnlineFirst November 19, 2010; DOI:10.1158/1078-0432.CCR-10-1382

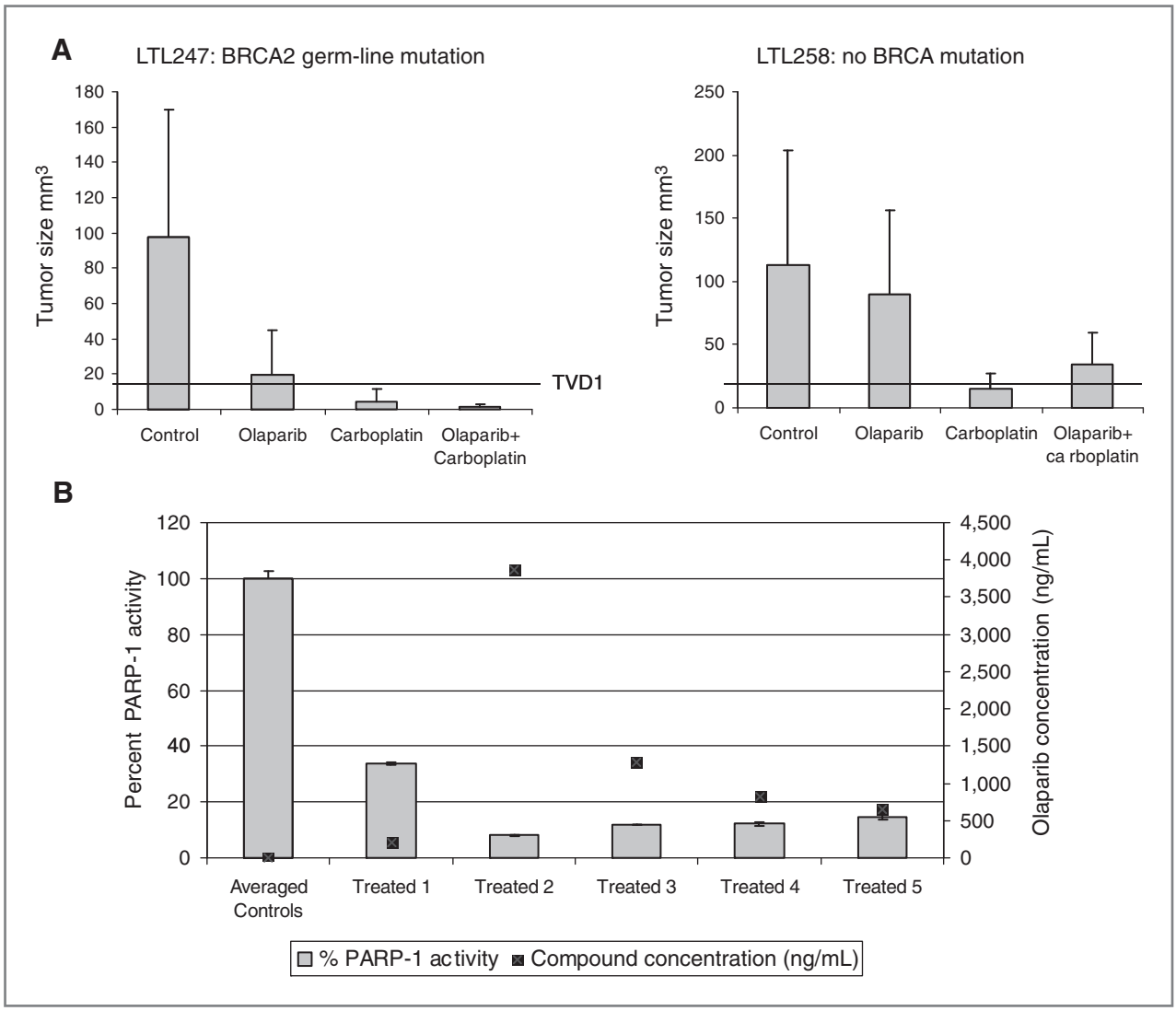

Figure 3. A, tumor growth inhibition. Left, *BRCA2*$^{-/-}$ xenograft LTL247; right, *BRCA1*$^{+/+}$, *BRCA2*$^{+/+}$ wild-type xenograft LTL258 TVD1: calculated averaged tumor volume on first treatment day = 16.64 mm^3. B, PARP-1 activity and olaparib concentration in averaged controls and 5 randomly selected olaparib-treated tumors from LTL247$^{BRCA2-/-}$.

(SD) vs. 0.8% ± 0.5% (SD); $P = 0.006$]. In the *BRCA* competent tumor line, no significant difference in the AI between olaparib treated and untreated xenografts could be observed [0.7% ± 0.6% (SD) vs. 0.8% ± 0.9% (SD); $P = 0.8$; Fig. 4D, right and left].

In agreement with the caspase-3 assay, TUNEL stains of 6 representative olaparib-treated LTL247$^{BRCA2-/-}$ tissue sections (Supplementary Figs. 1A and B) equally displayed a significantly higher number of apoptotic cells compared with untreated control xenografts (Supplementary Figs. 1C and D). On an average, the AI per high-power field was 2.3-fold increased in the olaparib-treated tumors [5.4% ± 1.35% (SD) vs. 2.3% ± 1.0% (SD); $P = 7.6e\text{-}16$].

H&E staining of residual tumor tissues after treatment with carboplatin alone and in combination with olaparib revealed only scar tissue but no tumor cells. Accordingly, no further immunohistochemistry could be performed for those treatment groups.

PARP-1 activity is strongly inhibited in olaparib-treated *BRCA2*$^{-/-}$ tumors and correlates with compound levels

Pharmacodynamic activity assays showed that all olaparib-treated tumors had greatly reduced PARP-1 activity compared with the average of vehicle-treated controls. On average, PARP-1 activity in olaparib-treated tumors was reduced to 16.1% (range 8.16%–33.75%; SD 10.1%) of untreated controls (100%). Untreated control tumors did not show detectable compound levels, whereas in olaparib-treated tumors, compound concentration ran-

Published OnlineFirst November 19, 2010; DOI:10.1158/1078-0432.CCR-10-1382

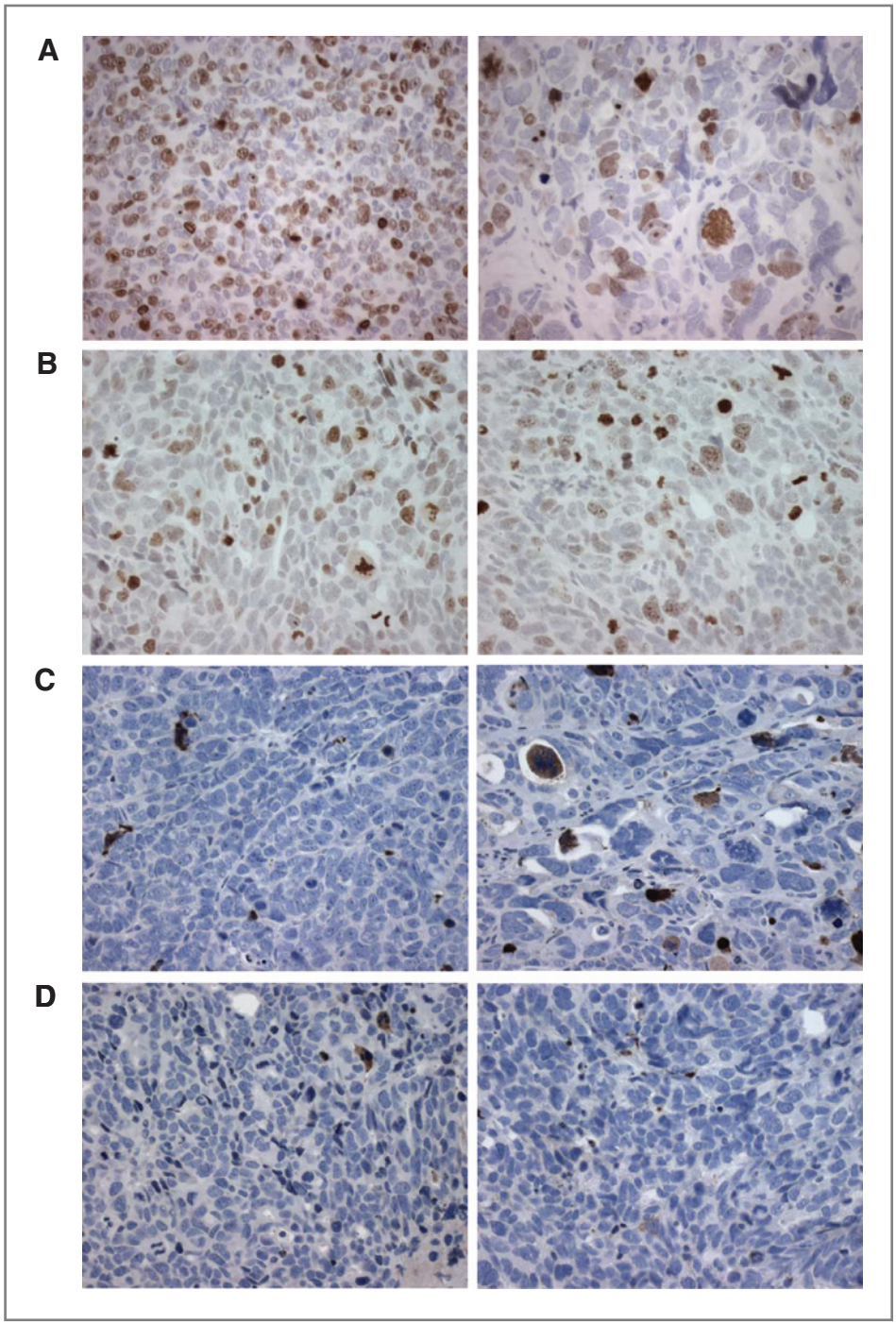

Figure 4. Ki-67 staining (400× magnification) of tumor sections. A, *BRCA2*$^{-/-}$ xenograft LTL247. Left, untreated control; right, olaparib-treated. B, *BRCA1*$^{+/+}$, *BRCA2*$^{+/+}$ wild-type xenograft LTL258. Left, untreated control; right, olaparib-treated cleaved caspase-3 staining (400× magnification of tumor sections. C, *BRCA2*$^{-/-}$ xenograft LTL247. Left, untreated control; right, olaparib-treated. D, *BRCA1*$^{+/+}$, *BRCA2*$^{+/+}$ wild-type xenograft LTL258. Left, untreated control; right, olaparib-treated.

ged from 198 to 3870 ng/mL with compound levels correlating well with PARP-1 activity (Pearson correlation 0.89; Fig. 3B).

Discussion

Using a patient-derived ovarian cancer xenograft model, we have demonstrated that *BRCA2* germline-mutated tumors are sensitive to single agent treatment with the PARP inhibitor olaparib. Although carboplatin showed better single agent efficacy, olaparib treatment also induced a clear tumor growth inhibition. This was in contrast to *BRCA* wild-type tumors, supporting findings in preclinical studies and early clinical trials that *BRCA* deficient tumors are susceptible to a synthetic lethal therapeutic approach (14–16). Furthermore, in most of the

Published OnlineFirst November 19, 2010; DOI:10.1158/1078-0432.CCR-10-1382

cases, combining olaparib with carboplatin either eradicated the tumors completely or left very small tumors which showed only scar tissue on microscopical inspection.

Notably, the addition of the PARP-inhibitor to carboplatin did not increase toxicity in mice.

Our results are in agreement with other studies that have tested olaparib in *BRCA1*$^{-/-;p53-/-}$ and *BRCA2*$^{-/-;p53-/-}$ genetically altered mouse models (17, 18). In these studies, the authors observed *in vivo* efficacy of olaparib (AZD2281) against *BRCA*-associated murine breast cancers with improvements in both recurrence-free and overall survival. We show, for the first time, that olaparib confers antitumor activity and improved survival in an experimental model utilizing human ovarian tumor tissue xenografts. Obvious differences between these models include variation of the genetic backgrounds across species, altered host immune responses, and the tissues studied. However, the comparability of the results further supports the efficacy of olaparib in these models independent of these parameters.

PARP inhibitors are currently being tested in various phase I/II clinical trials (7) and another PARP-inhibitor compound (BSI-201) is being investigated in a phase III trial of triple negative breast cancer (www.clinicaltrials.gov NCT00938652). In the case of olaparib, Fong and coworkers have recently reported on the pharmacokinetics and pharmacodynamics of this drug in a phase I clinical trial involving patients with cancers associated with *BRCA* mutations (including 16 patients with ovarian cancer; ref. 14). The authors observed antitumor activity only in *BRCA* mutation carriers and concluded that olaparib was effective in this subgroup with few side effects compared with conventional chemotherapy. Subsequent phase II trials of olaparib in *BRCA* mutation carriers with chemoresistant breast or ovarian cancer have been completed and preliminary results presented show high activity in those patients and an acceptable tolerability profile (22, 23). The suggestion has been made by others that combination therapy with PARP inhibitors amplifies cytotoxic effects of drugs such as carboplatin (17). In our study, the addition of olaparib to carboplatin in the *BRCA2* deficient tumor line did result in smaller tumors than single agent therapy, but the difference did not reach statistical significance (*t*-test *P*-value 0.07).

Furthermore, tumor relapse could be delayed in a mouse model by continuous treatment with olaparib alone after carboplatin chemotherapy, suggesting a role for olaparib in maintenance therapy during remissions (17, 18). It is possible that development of resistance to PARP inhibitors will hamper further clinical progress. Therefore, model systems that allow for the study of drug resistance would be useful. Here, we showed that a human ovarian cancer tissue explant xenograft mouse model has utility for the testing of experimental drugs in *BRCA*-mutated tumors. In the future, development of additional tumor tissue lines, including those that progressed under treatment, has the potential to elucidate the underlying molecular mechanisms of olaparib drug resistance.

In conclusion, this study shows the applicability of a xenograft model for experimental drug testing in human *BRCA*$^{-/-}$ ovarian tumors. To our knowledge, we are the first to develop a model for *BRCA2* deficiency directly derived from a patient's tumor. The efficacy of olaparib as a single agent or in combination with carboplatin warrants further investigation in clinical trials.

Disclosure of Potential Conflicts of Interest

A. Lau and M.J. O'Connor report being employees of AstraZeneca. A.N. Cranston as well as S. Tully and S. Shafait report having been employed by KuDOS Pharmaceuticals at the time experiments were performed. No other potential conflict of interest relevant to this article was reported.

Grant Support

This study was supported by NCIC (C.B. Gilks) and funding from OvCaRe (an initiative of the Vancouver General Hospital & University of BC Hospital Foundation and the BC Cancer Foundation) (D.G. Huntsman and Y.Z. Wang), the BC Cancer Foundation and AstraZeneca Plc. (Investigator-initiated project D.G. Huntsman).

The costs of publication of this article were defrayed in part by the payment of page charges. This article must therefore be hereby marked *advertisement* in accordance with 18 U. S. C. Section 1734 solely to indicate this fact.

Received May 21, 2010; revised October 29, 2010; accepted November 2, 2010; published OnlineFirst November 19, 2010.

References

1. Jemal A, Siegel R, Ward E, Hao Y, Xu J, Murray T, et al. Cancer statistics, 2008. CA Cancer J Clin 2008;58:71–96.
2. Russo A, Calo V, Bruno L, Rizzo S, Bazan V, Di Fede G. Hereditary ovarian cancer. Crit Rev Oncol Hematol 2009;69:28–44.
3. Turner N, Tutt A, Ashworth A. Hallmarks of 'BRCAness' in sporadic cancers. Nat Rev Cancer 2004;4:814–9.
4. Press JZ, De Luca A, Boyd N, Young S, Troussard A, Ridge Y, et al. Ovarian carcinomas with genetic and epigenetic BRCA1 loss have distinct molecular abnormalities. BMC Cancer 2008;8:17.
5. Tan DS, Rothermundt C, Thomas K, Bancroft E, Eeles R, Shanley S, et al. "BRCAness" syndrome in ovarian cancer: a case-control study describing the clinical features and outcome of patients with epithelial ovarian cancer associated with BRCA1 and BRCA2 mutations. J Clin Oncol 2008;26:5530–6.
6. Gudmundsdottir K, Ashworth A. The roles of BRCA1 and BRCA2 and associated proteins in the maintenance of genomic stability. Oncogene 2006;25:5864–74.
7. Lord CJ, Ashworth A. Targeted therapy for cancer using PARP inhibitors. Curr Opin Pharmacol 2008;8:363–9.
8. Plummer ER. Inhibition of poly(ADP-ribose) polymerase in cancer. Curr Opin Pharmacol 2006;6:364–8.
9. Menear KA, Adcock C, Boulter R, Cockcroft XL, Copsey L, Cranston A, et al. 4-[3-(4-cyclopropanecarbonylpiperazine-1-carbonyl)-4-fluorobenzyl]-2H-phthalazin-1-one: a novel bioavailable inhibitor of poly(ADP-ribose) polymerase-1. J Med Chem 2008;51:6581–91.
10. McGuire WP, 3rd, Markman M. Primary ovarian cancer chemotherapy: current standards of care. Br J Cancer 2003;89(Suppl 3):S3–8.

Published OnlineFirst November 19, 2010; DOI:10.1158/1078-0432.CCR-10-1382

11. Quinn JE, Carser JE, James CR, Kennedy RD, Harkin DP. BRCA1 and implications for response to chemotherapy in ovarian cancer. Gynecol Oncol 2009;113:134–42.
12. Ratnam K, Low JA. Current development of clinical inhibitors of poly (ADP-ribose) polymerase in oncology. Clin Cancer Res 2007; 13:1383–8.
13. Plummer R, Jones C, Middleton M, Wilson R, Evans J, Olsen A, et al. Phase I study of the poly(ADP-ribose) polymerase inhibitor, AG014699, in combination with temozolomide in patients with advanced solid tumors. Clin Cancer Res 2008;14:7917–23.
14. Fong PC, Boss DS, Yap TA, Tutt A, Wu P, Mergui-Roelvink M, et al. Inhibition of poly(ADP-ribose) polymerase in tumors from BRCA mutation carriers. N Engl J Med 2009;361:123–34.
15. Farmer H, McCabe N, Lord CJ, Tutt AN, Johnson DA, Richardson TB, et al. Targeting the DNA repair defect in BRCA mutant cells as a therapeutic strategy. Nature 2005;434:917–21.
16. Bryant HE, Schultz N, Thomas HD, Parker KM, Flower D, Lopez E, et al. Specific killing of BRCA2-deficient tumours with inhibitors of poly(ADP-ribose) polymerase. Nature 2005;434:913–7.
17. Rottenberg S, Jaspers JE, Kersbergen A, Van Der Burg E, Nygren AO, Zander SA, et al. High sensitivity of BRCA1-deficient mammary tumors to the PARP inhibitor AZD2281 alone and in combination with platinum drugs. Proc Natl Acad Sci U S A 2008;105:17079–84.
18. Hay T, Matthews JR, Pietzka L, Lau A, Cranston A, Nygren AO, et al. Poly(ADP-ribose) polymerase-1 inhibitor treatment regresses autochthonous Brca2/p53-mutant mammary tumors *in vivo* and delays tumor relapse in combination with carboplatin. Cancer Res 2009;69:3850–5.
19. Lee CH, Xue H, Sutcliffe M, Gout PW, Huntsman DG, Miller DM, et al. Establishment of subrenal capsule xenografts of primary human ovarian tumors in SCID mice: potential models. Gynecol Oncol 2005;96:48–55.
20. Shah SP, Xuan X, DeLeeuw RJ, Khojasteh M, Lam WL, Ng R, et al. Integrating copy number polymorphisms into array CGH analysis using a robust HMM. Bioinformatics 2006;22: e431–9.
21. Bengtsson H, Wirapati P, Speed TP. A single-array preprocessing method for estimating full-resolution raw copy numbers from all affymetrix genotyping arrays including GenomeWideSNP 5 & 6. Bioinformatics 2009;25:2149–56.
22. Audeh MW, Carmichael J, Penson RT, Friedlander M, Powell B, Bell-McGuinn KM, et al. Oral poly(ADP-ribose) polymerase inhibitor olaparib in patients with BRCA1 or BRCA2 mutations and recurrent ovarian cancer: A proof-of-concept trial. Lancet. 2010;376:245–51.
23. Tutt A, Robson M, Garber JE, Domchek SM, Audeh MW, Weitzel JN, et al. Oral poly(ADP-ribose) polymerase inhibitor olaparib in patients with BRCA1 or BRCA2 mutations and advanced breast cancer: A proof-of-concept trial. Lancet. 2010;376:235–44.